European Journal of Medicinal Chemistry 92 (2015) 115–123

Contents lists available at ScienceDirect

European Journal of Medicinal Chemistry

journal homepage: http://www.elsevier.com/locate/ejmech

Original article

Structure-based design of phthalimide derivatives as potential cyclooxygenase-2 (COX-2) inhibitors: Anti-inflammatory and analgesic activities

Amer M. Alanazi [a], Adel S. El-Azab [a, b], Ibrahim A. Al-Suwaidan [a], Kamal Eldin H. ElTahir [c], Yousif A. Asiri [d], Naglaa I. Abdel-Aziz [e], Alaa A.-M. Abdel-Aziz [a, e, *]

[a] Department of Pharmaceutical Chemistry, College of Pharmacy, King Saud University, Riyadh 11451, Saudi Arabia
[b] Department of Organic Chemistry, Faculty of Pharmacy, Al-Azhar University, Cairo 11884, Egypt
[c] Department of Pharmacology, College of Pharmacy, King Saud University, Riyadh 11451, Saudi Arabia
[d] Department of Clinical Pharmacy, College of Pharmacy, King Saud University, Riyadh 11451, Saudi Arabia
[e] Department of Medicinal Chemistry, Faculty of Pharmacy, University of Mansoura, Mansoura 35516, Egypt

ARTICLE INFO

Article history:
Received 19 September 2014
Received in revised form
22 December 2014
Accepted 23 December 2014
Available online 24 December 2014

Keywords:
Phthalimides
COX-2 inhibitors
Anti-inflammatory activity
Analgesic activity
Molecular docking

ABSTRACT

A group of 30 cyclic imides (**1**–**10a-c**) was designed for evaluation as a selective COX-2 inhibitor and investigated *in vivo* for anti-inflammatory and analgesic activities. Compounds **6a**, **6b**, **7a** and **7b** exhibit optimal COX-2 inhibitory potency (IC_{50} = 0.18, 0.24, 0.28 and 0.36 μM; respectively) and selectivity index (SI) range of 363–668. *In vitro* COX-1/COX-2 inhibition structure–activity studies identified compound **6a** as a highly potent (IC_{50} = 0.18 μM), and an extremely selective [COX-2 (SI) = 668] comparable to celecoxib [COX-2 (SI) > 384], COX-2 inhibitor that showed superior anti-inflammatory activity (ED_{50} = 54.0 mg/kg) relative to diclofenac (ED_{50} = 114 mg/kg). Molecular Docking study of the synthesized compound **6a** into the active site of COX-2 revealed a similar binding mode to SC-558, a selective COX-2 inhibitor. Docking study showed that the methoxy moeities of **6a** inserted deep inside the 2°-pocket of the COX-2 active site, where the O-atoms of such groups underwent an H-bonding interaction with His^{90} (3.02 Å), Arg^{513} (1.94, 2.83 Å), and Gln^{192} (3.25 Å).

© 2014 Elsevier Masson SAS. All rights reserved.

1. Introduction

Nonsteroidal anti-inflammatory drugs (NSAIDs) are the most important class of widely used therapeutics for the treatment of inflammation and pain [1,2]. The clinical use of traditional NSAIDs for the treatment of inflammation and pain is often accompanied by adverse gastrointestinal effects [1–3]. The pharmacological effects of NSAIDs are due to inhibition of a membrane enzyme called cyclooxygenase (COX) which is involved in the prostaglandin biosynthesis [4–13]. There are two isoforms, COX-1 and COX-2 which share the same substrates, produce the same products and catalyze the same reaction using identical catalytic mechanisms, but differ in inhibitor selectivity [4–9]. The isoform, COX-1 has mainly a physiological role in kidneys and the stomach, and is responsible for maintaining homeostasis (gastric and renal integrity) [7–9]. Whereas COX-2 induces inflammatory conditions and is involved in the production of prostaglandins mediating pain [10,11]. Inhibition of COX-1 is responsible for the adverse gastrointestinal and renal effects of NSAIDs while the inhibition of COX-2 accounts for NSAIDs' therapeutic effects. All classical NSAIDs, such as aspirin and indomethacin are non selective inhibitors for both COX-1 and COX-2, but bind more tightly to COX-1. In order to prevent or decrease these side effects, a current strategy consists of designing selective COX-2 inhibitors with an improved gastric safety profile [14,15]. Several classes of compounds possessing selective COX-2 inhibitory activity have been reported in the literature such celecoxib (**A**) and SC-558 (**B**) (Fig. 1) [16,17].

On the other hand, cyclic imides such as phthalimides possessed structural features which conferred potential biological activity and pharmaceutical use [18–21]. The various classes of cyclic imides have received great attention due to their COX-1/2 inhibition, anti-inflammatory, antihyperlipidemic and antitumor activities [18–23]. Apart from biological activities; imide derivatives are

* Corresponding author. Department of Pharmaceutical Chemistry, College of Pharmacy, King Saud University, Riyadh 11451, Saudi Arabia.
E-mail address: alaa_moenes@yahoo.com (A.A.-M. Abdel-Aziz).

http://dx.doi.org/10.1016/j.ejmech.2014.12.039
0223-5234/© 2014 Elsevier Masson SAS. All rights reserved.

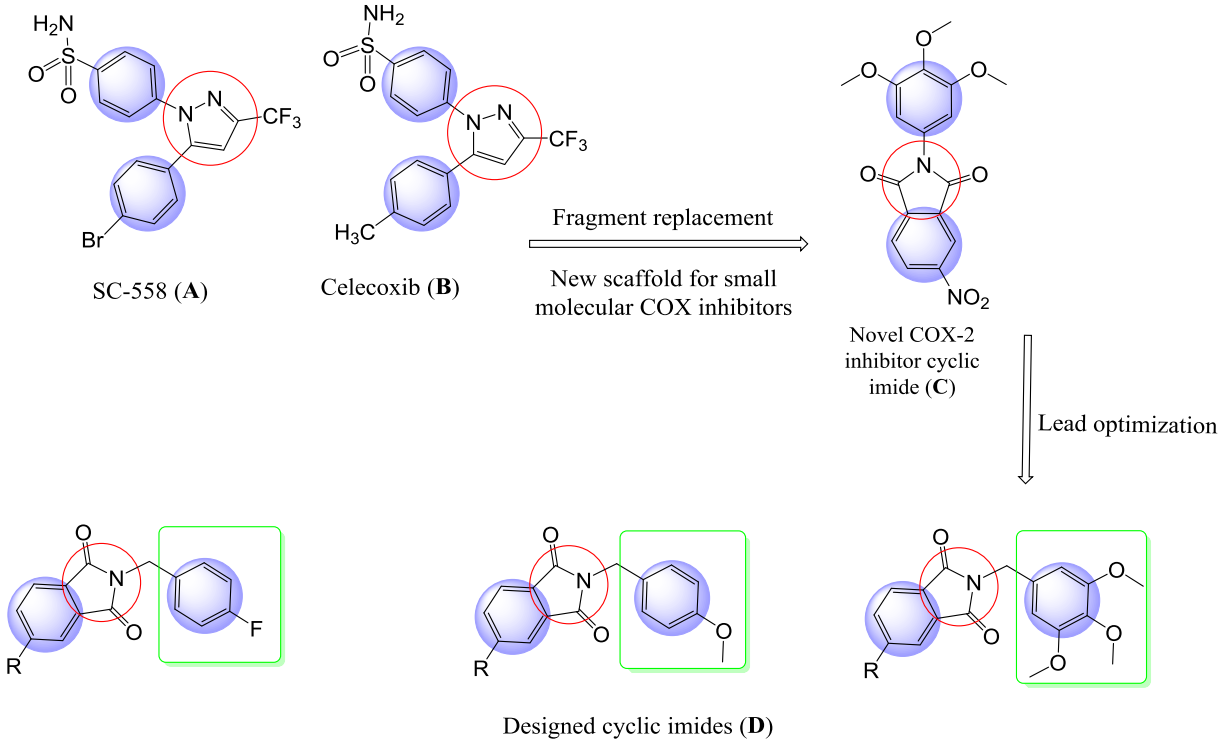

Fig. 1. Representative examples of selective COX-2 inhibitors (**A**, **B** and **C**) and the designed cyclic imides (**D**).

useful in the reactions involving condensation, alkylation, acylation, and cyclocondensation [24].

We have recently reported on the synthesis and COX-2-inhibiton of N-substituted cyclic imides [21,22] in which compound **C** (Fig. 1) was proved to be potent COX-2 inhibitors with IC_{50} value of 0.10 μM and an extremely selective [COX-2 (SI) = 400] [21]. Accordingly, we now describe the synthesis, COX-1/2 inhibition, anti-inflammatory and analgesic activities of a group of cyclic imides **1**–**10a-c** bearing 3,4,5-timethoxybenzyl, 4-methoxybenzyl, or 4-fluorobenzyl fragments, in conjunction with various substituents (H, Me, NO_2, Cl and *t*-butyl) at the cyclic imide core. The rationale for testing of these cyclic imides (Fig. 1, **D**) as COX-inhibitors was the following: (i) compare the efficacy of the 3,4,5-trimethoxybenzyl and 4-methoxybenzyl versus the 4-fluorobenzyl for the inhibitory power against various isoforms, such as COX-1 and COX-2, in compounds incorporating the same scaffold (i.e., succinimide; phthalimide, etc.); (ii) delineate the structure–activity relationship (SAR) for the inhibition of these COX isoforms with compounds incorporating cyclic imides with diversely substituted scaffolds. Thus, in addition to the monocyclic succinimide **(1a-c)**, derivatives of tetrahydrophthalimide (**2a-c**), phthalimide (**3a-c**) as well as phthalimide substituted with various moieties at the benzene core (such as methyl-, *tert*-butyl-, dichloro-, tetrachloro- and nitro-groups) of types **4-8a-c** were also included in the study. Furthermore, derivatives incorporating the heterocyclic pyrazine-2,3-dicarboximide **(9a-c)** or the bulkier naphthalene-1,10-dicarboximide (**10a-c**) moieties were also included in the study, in order to explore as much chemical space as possible.

2. Results and discussion

2.1. Chemistry

The preparation of target cyclic imides is shown in Scheme 1. Classical condensation of 3,4,5-trimethoxybenzyl amine or 4-substituted benzyl amine with an acid anhydride in refluxing acetic acid afforded the designed cyclic imides in satisfactory yields. The structures of the isolated products **1**–**10a-c** were established on the basis of their spectral analyses.

2.2. Biological activity

2.2.1. COX inhibition

According to the aforementioned rationale, the synthesized compounds are evaluated for their ability to inhibit COX-1 and COX-2 using an ovine COX-1/COX-2 assay kit (Catalog No. 560101, Cayman Chemicals Inc., Ann Arbor, MI, USA). IC_{50} (μM) is determined which is the means of two determinations acquired and the deviation from the mean is <10% of the mean value [21,22,25]. The selectivity index (SI values) was defined as IC_{50}(COX-1)/IC_{50}(COX-2). In the assay system, the IC_{50} values of celecoxib on COX-1 and COX-2 were determined to be > 100 and 0.26 μM respectively, indicating that celecoxib is a selective COX-2 inhibitor [COX-2 (SI) > 384.6]. The results showed that some of the tested compounds had potent inhibition against COX-2 ($IC_{50} \cong$ 0.18–8.5 μM) compared to the inhibition for COX-1 ($IC_{50} \cong$ 130.8 − >100 μM) as listed in Table 1. Nearly seven of the tested compounds (**6a**, **6b**, **7a**, **7b**, **8b**, **9a**, and **10a**) were found to be potent and selective against COX-2. Interestingly, methoxy substituents on the *N*-benzyl group play critical roles in the COX-inhibiting activity of the tested compounds compared with fluoro derivatives.

Compound **6a** was the most potent inhibitor in this series with the COX-2 inhibiting activity (IC_{50} = 0.18 μM, COX-2 (SI) = 668.3), 2-fold higher than celecoxib (IC_{50} = 0.26 μM, COX-2 (SI) > 384.6). The effects of substituents introduced into the phthaloyl moiety of compounds **3**–**8** were revealed to be directional, being dependent on the electronic nature of the substituents, that is introduction of a nitro group at the 5-position (compound **6a**) enhanced COX-2-inhibiting activity, resulting in a COX-2-selective inhibition (SI = 668.3). Moreover, introduction of two halogen atoms such as

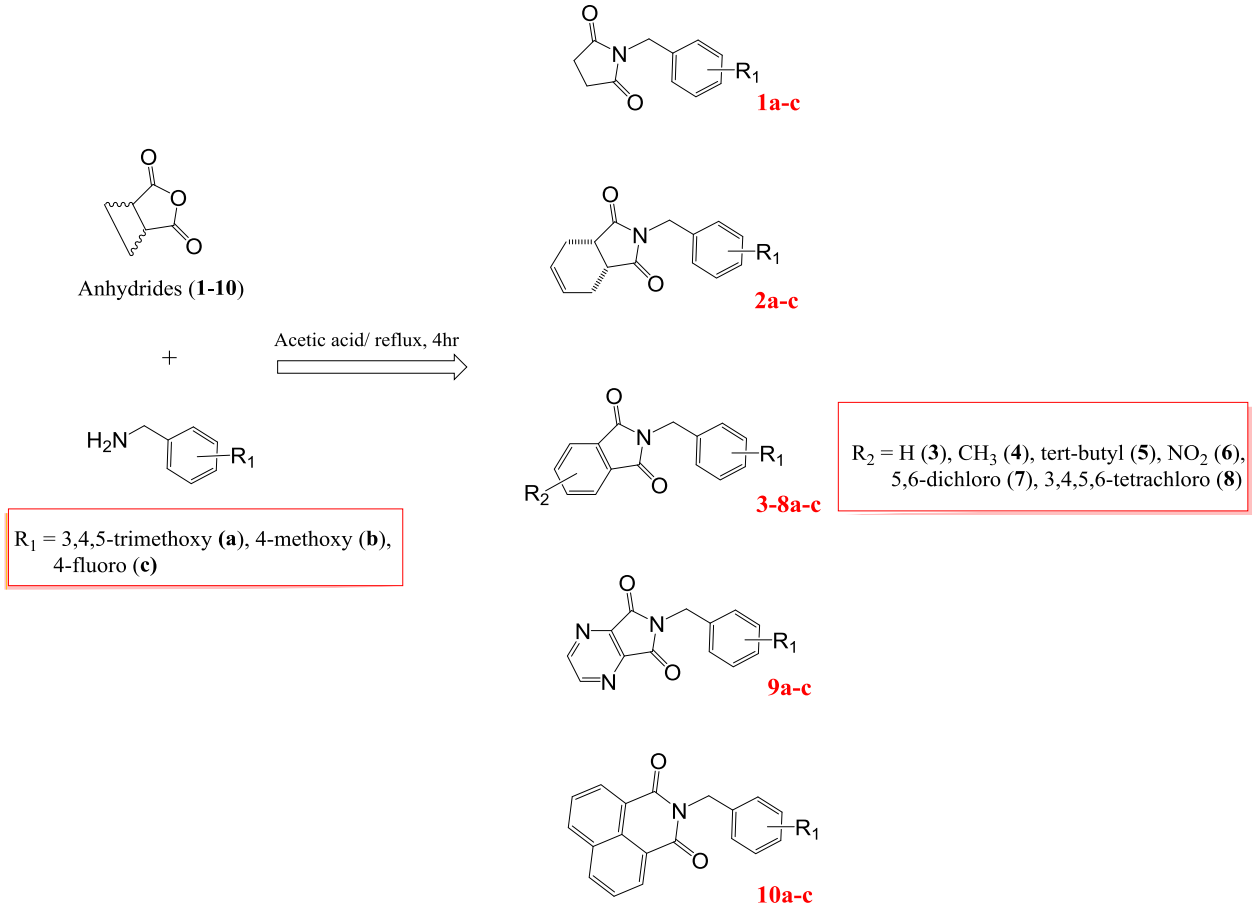

Scheme 1. Synthesis of the designed substituted cyclic imides **1**–**10**.

dichloro derivative (compounds **7a-b**) resulted in increasing the COX-2-inhibitory activity, while introduction of an electron-donating methyl or *tert*-butyl groups such as compounds **4** and **5** showed just the opposite effects, resulting in sharp decrease of a COX-2 inhibition. The activities of some other cyclic imides analogs (compounds **9**–**10**) are shown in Table 1, among them, compounds **9a** and **10a-b** are a COX-2-selective inhibitor (SI= >5.8–13.7). Diminishment of activity of compounds **1** and **2** may be explained on the bases of non-aromatic feature of the imide scaffold indicating the importance of aromatic fragment of imide core for the activity. More interestingly, fluoro substituents on the *N*-benzyl moiety showed loss or lower of COX-2 inhibition (compounds **1**–**10c**) when compared with methoxy substituents (compounds **1**–**10a-b**).

The following SAR was observed for the inhibition of the COX-2 isoform mentioned above with derivatives **1**–**10a-c** (Table 1): (i) The COX-2 isoform was well inhibited by many of the investigated compounds, such as **4a, 6a**, **6b**, **7a**, **7b**, **8b**, **9a**, **10a**, and **10b**, which showed IC_{50} (μM) ranging between 0.18 and 24.0, some of them showed more inhibitory than the standard drug celecoxib (IC_{50} of 0.26 μM). It may be observed that both 3,4,5-trimethoxy and 4-methoxybenzyl derivatives belong to this category of effective COX-2 inhibitors, while 4-fluorobenzyl seems to have been of little importance for the biological activity. For example the 3,4,5-trimethoxy and 4-methoxybenzyl pairs incorporating the same scaffolds (5-nitrophthalimide and 5,6-dichlorophthalimide) **6a/6b** and **7a/7b**, show similar inhibitory activity against COX-2 isoform, suggesting a quite similar binding mode to the enzyme. However other pairs differ considerably in their activity. For example the succinimide derivatives (**1a** and **1b**), the tetrahydrophthalimides (**2a** and **2b**), the tetrachlorophthalimides (**8a** and **8b**) or the heterocyclic pyrazineimides (**9a** and **9b**), show different inhibition profiles where the non-aromatic imides are much weaker inhibitors compared to the corresponding aromatic imides. For the two different methoxy derivatives, generally the 3,4,5-trimethoxy derivatives were slightly more inhibitory compared to the corresponding 4-methoxy derivatives, but the differences of activity were rather small (Table 1). It may be noted that diverse cyclic imide scaffolds lead to a highly efficient COX-2 inhibitors and the scaffolds leading to the best inhibition were just the 5-nitrophthalimide and 5,6-dichlorophthalimide (compounds **6a-b** and **7a**) which in fact possessed higher COX-2-selective inhibition (SI = 430–668) when compared with lead compound **C** reported earlier (SI = 400) [21].

2.2.2. *Anti-inflammatory activity*

Anti-inflammatory activity of twenty one compounds, which showed the specificity for COX-2 enzyme in the *in vitro* assay including compounds **1a**, **2a**, **3-4a-c**, **5a-b**, **6a-c**, **7a-b**, **8a-b**, and **9**–**10a-b**, was evaluated by employing the well-known rat carrageenan-induced foot paw oedema model (Table 2) [21,22,26]. The ED_{50} was measured after 2 h of treatment with carrageenan (Table 2), at which maximum percentage of inhibition of carrageenan-induced oedema was reached along with diclofenac sodium and celecoxib, as a reference drugs. All of the ED_{50} values were determined using three doses of 50, 100 and 200 mg/kg in the test compounds and 25, 50 and 100 mg/kg in the reference drugs diclofenac and celecoxib. Out of twenty one compounds, 10

Table 1
In vitro COX-1/COX-2 enzyme inhibition assay.

Compound No	IC_{50} (μM)[a]		SI[b]
	COX-1	COX-2	
1a	>100	75.1	>1.3
1b	>100	>100	>1.0
1c	>100	>100	>1.0
2a	>100	70.6	>1.4
2b	>100	>100	>1.0
2c	>100	>100	>1.0
3a	>100	33.8	>3.0
3b	110	40.1	2.7
3c	115.6	68.6	1.7
4a	>100	24.0	>4.2
4b	>100	36.1	>2.8
4c	>100	74.0	>1.4
5a	>100	32.2	>3.1
5b	>100	29.1	>3.4
5c	>100	>100	>1.0
6a	120.3	0.18	668.3
6b	118.6	0.24	494.2
6c	>100	31.1	>3.2
7a	120.4	0.28	430.0
7b	130.8	0.36	363.3
7c	>100	>100	>1.0
8a	>100	30.7	>3.3
8b	>100	4.1	>24.4
8c	>100	>100	>1.0
9a	>100	8.5	>11.8
9b	117.1	38.7	3.0
9c	>100	>100	>1.0
10a	>100	7.3	>13.7
10b	>100	17.1	>5.8
10c	>100	>100	>1.0
C	40.0	0.1	400.0
Diclofenac	0.25	4.2	0.06
Celecoxib	>100	0.26	>384.6

[a] IC_{50} value is the compound concentration required to produce 50% inhibition of COX-1or COX-2 for means of two determinations using an ovine COX-1/COX-2 assay kit (catalog no. 560101, Cayman Chemicals Inc., Ann Arbor, MI, USA) and deviation from the mean is <10% of the mean value.
[b] Selectivity index (COX-1 IC_{50}/COX-2 IC_{50}).

Table 2
In vivo anti-inflammatory activity against carrageenan-induced rat paw oedema and analgesic activity represented by ED_{50} (mg/kg) of the designed compounds.

Compound No	ED_{50}; mg/kg (mmol/kg)	
	AI[a]	Analgesic[b]
1a	180.0	95.0
2a	171.0	125.0
3a	149.0	109.9
3b	161.7	106.9
3c	170.0	90.0
4a	130.0	ND[c]
4b	153.0	80.5
4c	172.0	97.0
5a	147.0	79.3
5b	137.0	96.1
6a	54.0	27.6
6b	68.0	17.0
6c	127.4	35.0
7a	67.0	57.4
7b	75.0	51.2
8a	143.5	54.7
8b	103.0	52.9
9a	119.0	40.5
9b	159.3.0	106.3
10a	115.0	88.0
10b	129.0	119.0
Celecoxib	83.4	71.0

[a] Anti-inflammatory activity represented by ED_{50} which was the effective dose calculated after 2 h.
[b] Analgesic activity represented by ED_{50} which was the effective dose calculated after 60 min.
[c] Not determined.

compounds (**4a**, **6a**, **6b**, **6c**, **7a**, **7b**, **8b**, **9a**, **10a** and **10b**) were found to possess potent anti-inflammatory activity (ED_{50} of 54.0–130.0 mg/kg). Compound **6a** showed the highest anti-inflammatory activity among the tested compounds with ED_{50} of 54.0 mg/kg compared to diclofenac sodium (ED_{50} = 114 mg/kg).

In general, cyclic imides containing 4-methoxybenzyl moiety such as compounds **6b**, **7b, 8b** and **10b** have shown higher anti-inflammatory activity when compared with compounds containing 4-fluorobenzyl fragment at the same position (**6c**, **8b**, **9b** and **10b**). These findings may be attributed to the importance of methoxybenzyl fragment in COX receptor binding site. Briefly, in the carrageenan-induced rat paw oedema assay model, compound **6a** was the most potent anti-inflammatory agent (ED_{50} = 54.0 mg/kg) within this group of compounds at 2 h post-drug administration.

2.2.3. Analgesic activity

The analgesic activity of the same selected compounds was evaluated using the hot plate technique in mice after 60 min of intraperitoneal injection at 58 °C using celecoxib as a reference drug [27–29]. A comparative study of the analgesic activity of the test compounds relative to the reference drug at 60 min revealed the following: the highest analgesic activity was recorded for compounds **6a-c**, **7a-b**, **8a-b** and **9a** with ED_{50} of 27.6, 17.0, 35.0, 57.4, 51.2, 54.7, 52.9 and 40.5 mg/kg when compared with celecoxib (ED_{50} of 71.0 mg/kg) after 60 min, respectively, this might be contributed to the presence of methoxybenzyl fragments. Special high analgesic activity was displayed by compounds **6a-c**, which exhibited potent analgesic activity almost more than three times (17–35 mg/kg) as that of celecoxib (71.0 mg/kg). However, compounds **2a**, **3a-b**, **9b** and **10b** (ED_{50} of 125.0, 109.9, 106.9, 106.3 and 119.0 mg/kg, respectively) appeared to have lower analgesic activity in comparison with reference drug celecoxib.

2.3. Docking studies

Insights into the differences between the binding sites of COX-1 and COX-2 obtained from X-ray crystal structure data, provided useful guidelines that facilitated the design of the selective COX-2 inhibitors [30–33]. For example, the COX-2 binding site possesses an additional 2°-pocket that is absent in COX-1, which is highly relevant to the design of selective COX-2 inhibitors. This COX-2 2°-pocket arises due to a conformational change at Tyr^{355} that is attributed to the presence of Ile^{523} in COX-1 relative to Val^{523} having a smaller side chain in COX-2 [34,35]. It has also been reported that replacement of His^{513} in COX-1 by Arg^{513} in COX-2 plays a key role with respect to the H-bond network in the COX-2 binding site. Access of ligands to the 2°-pocket of COX-2 is controlled by histidine (His^{90}), glutamine (Gln^{192}), and tyrosine (Tyr^{355}) [34,35]. Interaction of Arg^{513} with the bound drug is a requirement for time dependent inhibition of COX-2 [34,35].

To understand the COX-inhibiting behavior of the synthesized compounds, automated docking studies were carried out using MOE 2008.10 software installed on 2.3G Core i7 [36]. The scoring function and a number of hydrogen bondings formed with the surrounding amino acids are used to predict their binding modes, binding affinities in the active sites of COX-2 enzyme. The level of COX-2 inhibition of compound **6a** prompted us to perform molecular docking studies to understand the ligand–protein interactions in detail. For this study, the crystal structures of COX-2 enzymes complexed with SC-558 [1CX2] were used for the docking [37]. The

active site of the enzyme was defined to include residues within a 10.0 Å radius to any of the inhibitor atoms and the scoring functions for docked compounds were calculated from minimized ligand–protein complexes. The most stable docking model was selected according to the best scored conformation predicted by the MOE scoring function. The compound **6a** could dock into the active site of COX-2 successfully (Fig. 2). Compound **6a** produces a deep moving into the hydrophilic pocket of COX-2 with which the methoxy groups are able to reach the hydrophilic pocket and is involved in hydrogen bonding with His^{90} (3.02 Å), Arg^{513} (1.94, 2.83 Å), and Gln^{192} (3.25 Å). Such interactions are almost essential for COX-2 inhibitory activity, as exemplified by the binding interaction of SC-558, an analog of celecoxib cocrystallized in the COX-2 active site [37]. In addition; such interaction forces the imide core to adopt a specific orientation at the top of the channel. This moiety is involved in hydrophobic interaction with Trp^{387}, Val^{523}, Leu^{352} and Phe^{518}. Moreover the two carbonyl moieties of the imide core and the 5-nitro group were forming hydrogen bonds with Ala^{527} (3.03 Å), Val^{349} (2.70 Å), Gly^{526} (2.08 Å) and Tyr^{385} (2.84 Å) respectively. The lateral pocket of COX-2 would therefore be responsible for the COX-2 selectivity of **6a** and contributed to stabilize the ligand–enzyme complexes (Fig. 2).

The complex generated by docking studies of **6a** with COX-2 and superimposition with the structure of the selective inhibitor, SC-558, co-crystallized with COX-2, illustrated in Fig. 2, shows that compound **6a** can bind in the active site of this enzyme in approximately similar fashion as the pyrazolic prototype (SC-558). Comparison of the interactions performed by SC-558 in the crystal and the docked structure of **6a** with COX-2 (Fig. 2) shows that the methoxy groups of **6a** hydrogen bonded to the amino acid residue Gln^{192}, His^{90} and Arg^{513}, similarly to the sulfonyl moiety of the pharmacophoric sulfonamide group pertaining to SC-558. Moreover, additional hydrogen bonds were observed among the carbonyl oxygen and Val^{349} and Ala^{527}, while NO_2 moiety hydrogen bonded with Gly^{526} and Tyr^{385}. Additionally, *N*-benzyl system are positioned in the same region as *p*-sulfonamido-phenyl ring of SC-558, while, the aromatic ring of imide core of compound **6a** is close to the *p*-Br-phenyl ring of SC-558, in the aromatic region of the active site lined by aromatic amino acid residues such as Phe^{518}, Tyr^{385} and Trp^{387}, among others. In short, the described interactions are typical of selective inhibitors of COX-2, confirming the molecular design of the reported class of anti-inflammatory imide derivatives [21,22].

3. Conclusion

A group of 30 cyclic imides was synthesized and screened for COX-1/COX-2 inhibition, anti-inflammatory and analgesic activities. Compounds which showed significant COX-2 inhibition were subjected to anti-inflammatory and analgesic studies. It was detected that both 3,4,5-trimethoxybenzyl and 4-methoxybenzyl derivatives were highly efficient COX-2 selective enzymes inhibitors compared to the 4-fluorobenzyl incorporating the same scaffold. Compounds **6a**, **6b**, **7a** and **7b** exhibit optimal COX-2 inhibitory potency (IC_{50} = 0.18, 0.24, 0.28 and 0.36 μM; respectively) and selectivity (SI) 363–668] comparable with celecoxib and better ED_{50} than diclofenac.

Molecular docking studies further help in understanding the various interactions between the ligands and enzyme active sites in detail and thereby help to design novel potent inhibitors. It is clear that the methoxy moieties of **6a** inserts deep inside the COX-2 2°-pocket and forming hydrogen bonds with His^{90} (3.02 Å), Arg^{513} (1.94, 2.83 Å), and Gln^{192} (3.25 Å). This result was corroborated by molecular docking studies with COX-2 inhibition, which showed that this compound presents the pharmacophoric requisites for COX-2 inhibition. Indeed molecular docking studies further supported the strong inhibitory activity of **6a** and further help understanding the various interactions between the ligands and enzyme active sites in detail and thereby help to design novel potent inhibitors.

4. Experimental

4.1. Chemistry

Melting points (uncorrected) were recorded on Barnstead 9100 Electrothermal melting apparatus. IR spectra were recorded on an FT-IR Perkin–Elmer spectrometer. ^1H NMR were recorded in DMSO-d6 on Bruker 500 and 700 MHz instruments using TMS as internal standard (chemical shifts in δ ppm) and ^{13}C NMR were

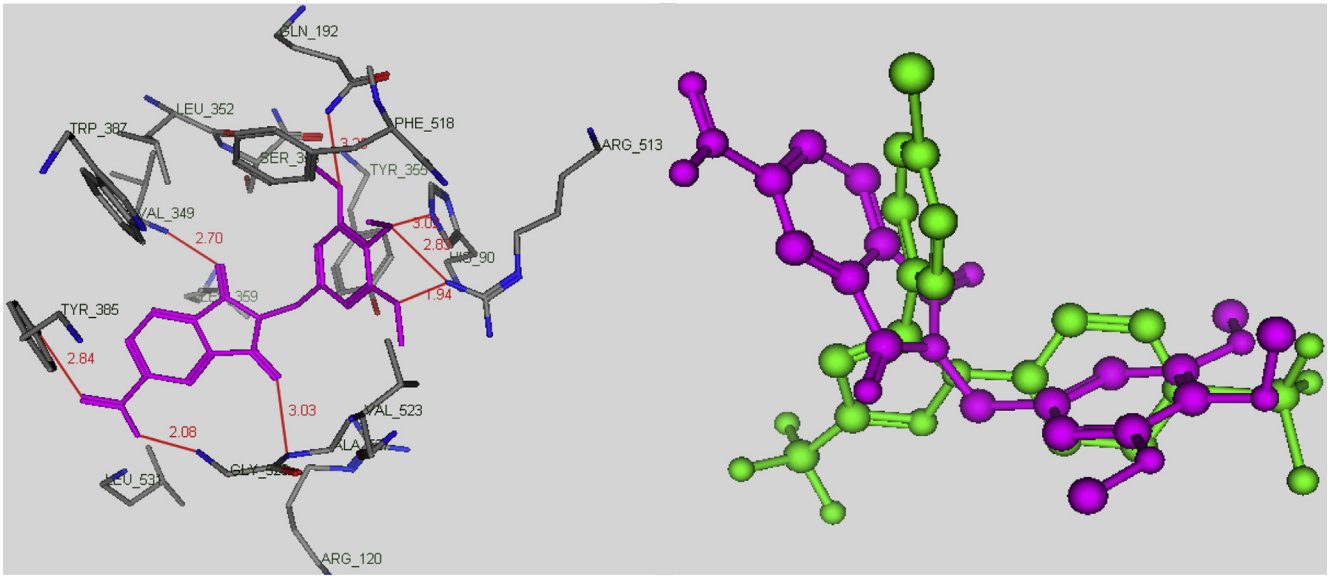

Fig. 2. Left panel showed docking of compound **6a** into the active site of COX-2. Hydrogen bonds are shown in red. Right panel showed alignment of **6a** (magenta) and selective inhibitor SC-558 (green) in the active site of COX-2. (For interpretation of the references to color in this figure legend, the reader is referred to the web version of this article.)

recorded in DMSO-d_6 on Bruker 125 and 176 MHz instruments using TMS as internal standard (chemical shifts in δ ppm). Mass spectra were recorded on a Agilent 6320 Ion Trap mass spectrometers. Elemental analysis was carried out for C, H and N at the Research Centre of College of Pharmacy, King Saud University and the results are within ±0.4% of the theoretical values. Solvent evaporation was performed under reduced pressure using Buchan Rotatory Evaporator unless otherwise stated. Thin layer chromatography was performed on precoated (0.25 mm) silica gel GF254 plates (E. Merck, Germany), compounds were detected with 254 nm UV lamp. Silica gel (60–230 mesh) was employed for routine column chromatography separations. Compounds **1b-c**, **2b**, **3b-c**, **6b-c**, **9b** and **10b-c** were prepared according to their reported procedure [20,38–47].

*4.1.1. General procedure for the synthesis of compounds **1–10***

A solution of substituted benzyl amine (10 mmol) and an acid anhydride (10 mmol) in glacial acetic acid (15 mL) was heated under reflux for 4 h. After the evaporation of the reaction mixture to dryness under reduced pressure, the residue was neutralised by a solution of sodium bicarbonate (4%) until effervescence ceased. The precipitate obtained was washed with water, dried and re-crystallised from an appropriate solvent.

*4.1.1.1. 1-(3,4,5-Trimethoxybenzyl)pyrrolidine-2,5-dione (**1a**).* White crystals, M.p 122–123°, 89% yield (CH_2Cl_2/CH_3OH); IR (KBr, cm^{-1}) ν: 1770, 1700 (C=O); ^{1}H NMR (DMSO-d_6): δ 2.69 (s, 4H), 3.62, (s, 3H), 3.74 (s, 6H), 4.47 (s, 2H), 6.55 (s, 2H); ^{13}C NMR: 28.06 ($2CH_2$), 41.47 (CH_2-Benzylic), 55.83 ($2CH_3O$), 59.90 (CH_3O), 105.13, 131.97, 136.85, 152.79, 177.60 (2C=O); $C_{14}H_{17}NO_5$: *m/z* (280.0). Anal. Calcd: C, 60.21; H, 6.14; N, 5.02. Founded: C, 60.96; H, 7.01; N, 4.19.

*4.1.1.2. 2-(3,4,5-Trimethoxybenzyl)-3a,4,7,7a-tetrahydro-1H-isoindole-1,3(2H)-dione (**2a**).* White crystals, M.p 147–148°, 93% yield (CH_2Cl_2/CH_3OH); IR (KBr, cm^{-1}) ν: 1777, 1704 (C=O); ^{1}H NMR (DMSO-d_6): δ 2.19–2.22 (d, 2H, J = 15 Hz), 2.44–2.47 (d, 2H, J = 14.5 Hz), 3.23 (s, 2H), 3.61 (s, 3H), 3.71 (s, 6H), 4.48 (s, 2H), 5.91 (s, 2H), 6.57 (s, 2H); ^{13}C NMR: 23.12 ($2CH_2$), 38.63(2CH), 41.58 (CH_2-Benzylic), 55.75 (2 CH_3O), 59.91(CH_3O), 103.82, 127.89, 131.66, 136.46, 152.81, 180.03 (2C=O); $C_{18}H_{21}NO_5$: *m/z* (332.0). Anal. Calcd: C, 65.24; H, 6.39; N, 4.23. Founded: C, 65.80; H, 7.28; N, 4.30.

*4.1.1.3. 2-(4-Fluorobenzyl)-3a,4,7,7a-tetrahydro-1H-isoindole-1,3(2H)-dione (**2c**).* White crystals, M.p 75–77°, 78% yield (CH_2Cl_2/CH_3OH); IR (KBr, cm^{-1}) ν: 1767, 1695 (C=O); ^{1}H NMR (DMSO-d_6): δ 2.17–2.18 (t, 2H, J = 4.5 Hz), 2.20–2.17 (t, 2H, J = 4.5 Hz), 3.18–3.20 (t, 2H, J = 3.0 Hz), 4.46 (s, 2H), 5.85–5.86 (t, 2H, J = 3.0 Hz), 6.85–6.87 (d, 2H, J = 8.5 Hz), 7.10–7.12 (d, 2H, J = 8.5 Hz); ^{13}C NMR: 23.08 ($2CH_2$), 38.55 (2CH), 40.98 (CH_2-Benzylic), 113.76, 127.71, 128.10, 128.65, 158.47, 179.82 (2C=O); $C_{15}H_{14}FNO_2$: *m/z* (260.0). Anal. Calcd: C, 69.49; H, 5.44; N, 5.40. Founded: C, 69.89; H, 5.31; N, 5.30.

*4.1.1.4. 2-(3,4,5-Trimethoxybenzyl)isoindoline-1,3-dione (**3a**).* White powder, M.p 138–140°, 90% yield (CH_2Cl_2/CH_3OH); IR (KBr, cm^{-1}) ν: 1766, 1708 (C=O); ^{1}H NMR (DMSO-d_6): δ 3.61 (s, 3H), 3.72 (s, 6H), 4.69 (s, 2H), 6.617 (s, 2H), 7.86–7.88 (d, 4H, J = 13.5 Hz); ^{13}C NMR: 41.11(CH_2-Benzylic), 55.83 ($2CH_3O$), 59.93 (CH_3O), 104.95. 123.20, 131.50, 132.31, 134.52, 136.80, 152.86, 167.77 (2C=O); $C_{18}H_{17}NO_5$: *m/z* (328.0). Anal. Calcd: C, 66.05; H, 5.23; N, 4.28. Founded: C, 66.81; H, 5.42; N, 4.19.

*4.1.1.5. 5-Methyl-2-(3,4,5-trimethoxybenzyl)isoindoline-1,3-dione (**4a**).* White crystals, M.p 140–141°, 88% yield (CH_2Cl_2); IR (KBr, cm^{-1}) ν: 1768, 1700 (C=O); ^{1}H NMR (DMSO-d_6): δ 2.46 (s, 3H), 3.61 (s, 3H), 3.72 (s, 3H), 4.67 (s, 2H), 6.66 (s, 2H), 7.77–7.90 (m, 3H); ^{13}C NMR: 21.30 (CH_3), 41.02 (CH_2-Benzylic), 55.80 ($2CH_3O$), 59.92 (CH_3O), 104.87, 123.09, 123.60, 128.85, 131.84, 132.39, 134.81, 136.79, 145.48, 152.86, 167.71 (C=O), 167.82 (C=O); $C_{19}H_{19}NO_5$: *m/z* (341.9). Anal. Calcd: C, 66.85; H, 5.61; N, 4.10. Founded: C, 66.34; H, 5.58; N, 4.03.

*4.1.1.6. 2-(4-Methoxybenzyl)-5-methylisoindoline-1,3-dione (**4b**).* White powder, M.p 130–132°, 80% yield (CH_2Cl_2); IR (KBr, cm^{-1}) ν: 1765, 1701 (C=O); ^{1}H NMR (DMSO-d_6): δ 2.47 (s, 3H), 3.71 (s, 3H), 4.67 (s, 2H), 6.87–6.88 (d, 2H, J = 7.5 Hz), 7.23–7.24 (d, 2H, J = 7.5 Hz), 7.62–7.64 (d, 1H, J = 7.5 Hz), 7.70 (s, 1H), 7.74–7.76 (d, 1H, J = 7.5 Hz); ^{13}C NMR: 21.31(CH_3), 42.01(CH_2-Benzylic), 55.03 (CH_3O), 113.91, 123.04, 123.56, 128.74, 128.92, 131.86, 134.80, 145.45, 158.56, 167.61 (C=O), 167.70 (C=O); $C_{17}H_{15}NO_3$: *m/z* (282.0). Anal. Calcd: C, 72.58; H, 5.37; N, 4.98. Founded: C, 71.80; H, 5.30; N, 4.52.

*4.1.1.7. 2-(4-Fluorobenzyl)-5-methylisoindoline-1,3-dione (**4c**).* White crystals, M.p 125–126°, 92% yield (CH_2Cl_2/Hexane); IR (KBr, cm^{-1}) ν: 1767, 1702 (C=O); ^{1}H NMR (DMSO-d_6): δ 2.46 (s, 3H), 4.72 (s, 2H), 7.03–7.07 (q, 2H, J = 8.5 Hz), 7.32–7.35 (q, 2H, J = 8.5 Hz), 7.55–7.57 (d, 1H, J = 7.5 Hz), 7.63 (s, 1H), 7.69–7.70 (d, 1H, J = 7.5 Hz); ^{13}C NMR: 21.38 (CH_3), 39.09 (CH_2-Benzylic), 115.02, 115.19, 122.90, 123.47, 128.86, 129.61, 129.67, 131.84, 132.62, 132.64, 134.56, 145.18, 160.50, 162.45, 167.34 (C=O), 167.44 (C=O); $C_{16}H_{12}FNO_2$: *m/z* (270.0). Anal. Calcd: C, 71.37; H, 4.49; N, 5.20. Founded: C, 70.92; H, 4.16; N, 5.11.

*4.1.1.8. 5-(tert-Butyl)-2-(3,4,5-trimethoxybenzyl)isoindoline-1,3-dione (**5a**).* White powder, M.p 119–120°, 87% yield (CH_2Cl_2); IR (KBr, cm^{-1}) ν: 1765, 1704 (C=O); ^{1}H NMR (DMSO-d_6): δ 1.33 (s, 9H), 3.61 (s, 3H), 3.86 (s, 6H), 4.68 (s, 2H), 6.61 (s, 2H), 7.79–7.872 (q, 3H, J = 7.5, 8.0 Hz); ^{13}C NMR: 30.69 ($3CH_3$-*tert*-Butyl), 35.39 (C-*tert*-Butyl), 41.08 (CH_2-Benzylic), 55.83 ($2CH_3O$), 59.92 (CH_3O), 104.96, 119.97, 123.09, 128.98, 131.34, 131.80, 132.40, 136.81, 152.86, 158.21, 167.61 (C=O), 167.91 (C=O); $C_{22}H_{25}NO_5$: *m/z* (384.0). Anal. Calcd: C, 68.91; H, 6.57; N, 3.65. Founded: C, 68.82; H, 6.91; N, 3.63.

*4.1.1.9. 5-(tert-Butyl)-2-(4-methoxybenzyl)isoindoline-1,3-dione (**5b**).* White powder, M.p 106–107°, 79% yield (CH_2Cl_2); IR (KBr, cm^{-1}) ν: 1765, 1715 (C=O); ^{1}H NMR (DMSO-d_6): δ 1.32 (s, 9H), 3.70 (s, 3H), 4.68 (s, 2H), 6.86–6.87 (d, 2H, J = 8.5 Hz), 7.22–7.24 (d, 2H, J = 8.5 Hz), 7.78–7.79 (d, 1H, J = 8.0 Hz), 7.83–7.84 (d, 2H, J = 3.5 Hz); ^{13}C NMR: 30.68 ($3CH_3$-*tert*-Butyl), 35.38 (C-*tert*-Butyl), 40.24 (CH_2-Benzylic), 55.01 (CH_3O), 113.88, 119.94, 123.01, 128.73, 128.87, 128.98, 131.27, 131.79, 158.17, 158.55, 167.46 (C=O), 167.77 (C=O); $C_{20}H_{21}NO_3$: *m/z* (324.1). Anal. Calcd: C, 74.28; H, 6.55; N, 4.33. Founded: C, 73.34; H, 7.03; N, 4.12.

*4.1.1.10. 5-(tert-Butyl)-2-(4-fluorobenzyl)isoindoline-1,3-dione (**5c**).* White powder, M.p 80–82°, 77% yield (CH_2Cl_2/CH_3OH); IR (KBr, cm^{-1}) ν: 1772, 1717 (C=O); ^{1}H NMR (DMSO-d_6): δ 1.34 (s, 9H), 4.74 (s, 2H), 7.09 (s, 2H), 7.33–7.34 (t, 2H, J = 5.5 Hz), 7.79–7.84 (t, 3H, J = 6.0 Hz); ^{13}C NMR: 30.73 ($3CH_3$-*tert*-Butyl), 35.37 (C-*tert*-Butyl), 40.07 (CH_2-Benzylic), 115.09, 115.26, 119.97, 123.01, 128.96,129.52, 129.59, 131.20, 131.78, 132.77, 158.15, 160.47, 162.41, 167.35 (C=O), 167.66 (C=O); $C_{19}H_{18}FNO_2$: *m/z* (312.1). Anal. Calcd: C, 73.30; H, 5.83; N, 4.50. Founded: C, 72.89; H, 5.74; N, 4.50.

*4.1.1.11. 5-Nitro-2-(3,4,5-trimethoxybenzyl)isoindoline-1,3-dione (**6a**).* Yellow crystals, M.p 155–156°, 71% yield (CH_2Cl_2/CH_3OH); IR (KBr, cm^{-1}) ν: 1778, 1719 (C=O); ^{1}H NMR (DMSO-d_6): δ 3.64 (s, 3H), 3.77 (s, 6H), 4.72 (s, 2H), 6.67 (s, 2H), 8.07–8.08 (d, 1H, J = 8.0 Hz), 8.19–8.20 (d, 1H, J = 7.5 Hz), 8.28–8.29 (d, 1H, J = 8.0 Hz); ^{13}C NMR: 41.70 (CH_2-Benzylic), 55.90 ($2CH_3O$), 59.92 (CH_3O), 105.25, 105.48,

123.20, 126.96, 128.32, 131.72, 133.63, 136.12, 137.00, 144.34, 152.91, 163.19 (C=O), 165.91 (C=O); $C_{18}H_{16}N_2O_7$: *m/z* (372.9). Anal. Calcd: C, 58.07; H, 4.33; N, 7.52. Founded: C, 57.35; H, 4.59; N, 7.50.

*4.1.1.12. 5,6-Dichloro-2-(3,4,5-trimethoxybenzyl)isoindoline-1,3-dione (**7a**).* Yellow crystals, M.p 200–202°, 95% yield (CH_2Cl_2/CH_3OH); IR (KBr, cm^{-1}) ν: 1774, 1711 (C=O); ^1H NMR (DMSO-d_6): δ 3.61 (s, 3H), 3.72 (s, 6H), 4.69 (s, 2H), 6.61 (s, 2H), 8.19 (s, 2H); ^{13}C NMR: 41.47 (CH_2-Benzylic), 55.85 ($2CH_3O$), 59.93 (CH_3O), 104.90, 125.34, 131.58, 131.87, 136.82, 137.29, 152.87, 166.01 (2C=O); $C_{18}H_{15}Cl_2NO_5$: *m/z* (396.0). Anal. Calcd: C, 54.57; H, 3.82; N, 3.54. Founded: C, 54.50; H, 3.09; N, 3.47.

*4.1.1.13. 5,6-Dichloro-2-(4-methoxybenzyl)isoindoline-1,3-dione (**7b**).* White crystals, M.p 154–155°, 81% yield (CH_2Cl_2/CH_3OH); IR (KBr, cm^{-1}) ν: 1771, 1705 (C=O); ^1H NMR (DMSO-d_6): δ 3.75 (s, 3H), 4.69 (s, 2H), 6.88 (s, 2H), 7.25 (s, 2H), 8.21 (s, 2H); ^{13}C NMR: 41.23 (CH_2-Benzylic), 55.55 (CH_3O), 114.40, 125.83, 128.72, 129.55, 132.01, 137.81, 159.15, 166.38 (2C=O). Anal. Calcd for $C_{16}H_{11}Cl_2NO_3$: C, 57.17; H, 3.30; N, 4.17. Founded: C, 57.08; H, 3.21; N, 4.09.

*4.1.1.14. 5,6-Dichloro-2-(4-fluorobenzyl)isoindoline-1,3-dione (**7c**).* White crystals, M.p 165–166°, 84% yield (CH_2Cl_2/CH_3OH); IR (KBr, cm^{-1}) ν: 1771, 1736 (C=O); ^1H NMR (DMSO-d_6): δ 4.76 (s, 2H), 7.15 (s, 2H), 7.37 (s, 2H), 8.19 (s, 2H); ^{13}C NMR: 41.03 (CH_2-Benzylic), 115.74, 115.86, 125.87, 130.14, 130.19, 132.06, 132.93, 132.95, 137.83, 161.29, 162.67 (C=O), 166.39 (C=O). Anal. Calcd for $C_{15}H_8Cl_2FNO_2$: C, 55.58; H, 2.49; N, 4.32. Founded: C, 55.57; H, 2.06; N, 4.21.

*4.1.1.15. 4,5,6,7-Tetrachloro-2-(3,4,5-trimethoxybenzyl)isoindoline-1,3-dione (**8a**).* Yellow powder, M.p 205–206°, 89% yield (CH_3OH); IR (KBr, cm^{-1}) ν: 1778, 1719 (C=O); ^1H NMR (DMSO-d_6): δ 3.63 (s, 3H), 3.75 (s, 6H), 4.70 (s, 2H), 6.64 (s, 2H); ^{13}C NMR: 42.33 (CH_2-Benzylic), 56.45 ($2CH_3O$), 60.43 (CH_3O), 105.64, 128.59, 129.04, 131.94, 138.55, 153.38, 163.89 (2C=O). Anal. Calcd for $C_{18}H_{13}Cl_4NO_5$: C, 46.48; H, 2.82; N, 3.01. Founded: C, 47.09; H, 2.18; N, 3.47.

*4.1.1.16. 4,5,6,7-Tetrachloro-2-(4-methoxybenzyl)isoindoline-1,3-dione (**8b**).* White crystals, M.p 207–209°, 97% yield (CH_3OH); IR (KBr, cm^{-1}) ν: 1775, 1709 (C=O); ^1H NMR (DMSO-d_6): δ 3.73 (s, 3H), 4.70 (s, 2H), 6.89- 6.91 (d, 2H, J = 9.0 Hz), 7.27–7.29 (d, 2H, J = 8.5 Hz); ^{13}C NMR: 41.15 (CH_2-Benzylic), 54.83 (CH_3O), 125.84, 127.96, 128.16, 128.41, 138.16, 139.60, 143.30, 163.22 (2C=O); $C_{16}H_9Cl_4NO_3$: *m/z* (403.5). Anal. Calcd: C, 47.44; H, 2.24; N, 3.46. Founded: C, 47.49; H, 2.20; N, 3.47.

*4.1.1.17. 4,5,6,7-Tetrachloro-2-(4-fluorobenzyl)isoindoline-1,3-dione (**8c**).* White powder, M.p 230–231°, 91% yield (CH_3OH); IR (KBr, cm^{-1}) ν: 1774, 1716 (C=O); ^1H NMR (DMSO-d_6): δ 4.72 (s, 2H), 7.02–7.03 (d, 2H, J = 8.5 Hz), 7.32–7.35 (t, 2H, J = 7.5 Hz); ^{13}C NMR: 40.92 (CH_2-Benzylic), 115.04, 115.21, 127.95, 128.51, 129.96, 130.03, 131.60, 138.63, 162.89 (2C=O); $C_{15}H_6Cl_4FNO_2$: *m/z* (391.1). Anal. Calcd: C, 45.84; H, 1.54; N, 3.56. Founded: C, 46.22; H, 1.05; N, 3.59.

*4.1.1.18. 6-(3,4,5-Trimethoxybenzyl)-5H-pyrrolo[3,4-b]pyrazine-5,7(6H)-dione (**9a**).* White powder, M.p > 300°, 61% yield (CH_2Cl_2/CH_3OH); IR (KBr, cm^{-1}) ν: 1705 (C=O), 1629 (C=N); ^1H NMR (DMSO-d_6): δ 3.68 (s, 3H), 3.78 (s, 6H), 4.20 (s, 2H), 6.55 (s, 2H), 8.186 (s, 2H); ^{13}C NMR: 42.48 (CH_2-Benzylic), 55.68 ($2CH_3O$), 59.89 (CH_3O), 104.57, 134.96, 136.33, 152.68, 169.27 (C=O), 172.97 (C=O); $C_{16}H_{15}N_3O_5$: *m/z* (330.0). Anal. Calcd: C, 58.36; H, 4.59; N, 12.76. Founded: C, 58.70; H, 4.12; N, 12.16.

*4.1.1.19. 6-(4-Fluorobenzyl)-5H-pyrrolo[3,4-b]pyrazine-5,7(6H)-dione (**9c**).* White crystals M.p 105–106°, 67% yield (CH_2Cl_2/CH_3OH); IR (KBr, cm^{-1}) ν: 1772, 1707 (C=O), 1615 (C=N); ^1H NMR (DMSO-d_6): δ 4.80 (s, 2H), 7.59 (s, 2H), 7.89 (s, 2H) 8.17 (s, 2H); ^{13}C NMR: 40.44 (CH_2-Benzylic), 126.19, 129.46, 133.44, 134.68, 134.94, 150.92, 166.90 (C=O), 167.46 (C=O). Anal. Calcd for $C_{13}H_8FN_3O_2$: C, 60.70; H, 3.14; N, 16.34. Founded: C, 60.77; H, 3.21; N, 16.31.

*4.1.1.20. 2-(3,4,5-Trimethoxybenzyl)-1H-benzo[de]isoquinoline-1,3(2H)-dione (**10a**).* White crystals, M.p 170–171°, 79% yield (CH_2Cl_2); IR (KBr, cm^{-1}) ν: 1771, 1718 (C=O); ^1H NMR (DMSO-d_6): δ 3.614 (s, 3H), 3.716 (s, 6H), 5.18 (s, 2H), 6.699 (s, 2H), 7.87–7.93 (m, 2H), 8.52–8.56 (m, 4H); ^{13}C NMR: 43.12 (CH_2-Benzylic), 55.78 ($2CH_3O$), 59.84 (CH_3O), 105.27, 118.94, 121.92, 127.17, 127.46, 129.64, 130.88, 131.29, 132.36, 132.99, 134.39, 135.29, 136.65, 152.67, 160.60 (C=O), 163.48 (C=O); $C_{22}H_{19}NO_5$: *m/z* (378. 0). Anal. Calcd: C, 70.02; H, 5.07; N, 3.71. Founded: C, 70.03; H, 5.68; N, 3.60.

4.2. Biological assay

4.2.1. In vitro cyclooxygenase (COX) inhibition assay

The *in vitro* ability of test compounds and celecoxib to inhibit the COX-1 and COX-2 isozymes was carried out using Cayman colorimetric COX (ovine) inhibitor screening assay kit (kit catalog number 560101, Cayman Chemical, Ann Arbor, MI, USA) according to the manufacturer's instructions [21,22,25]. Briefly, to a series of supplied reaction buffer solutions (960 μL, 0.1 M Tris–HCl pH8.0 containing 5 μM EDTA and 2 μM phenol) with either COX-1or COX-2 (10 μL) enzyme in the presence of heme (10 μL) were added 10 μL of various concentrations of test drug solutions (0.01, 0.1, 1, 10, 50, and 100 μM in a final volume of 1 mL). These solutions were incubated for a period of 5 min at 37 °C after which 10 μL of Arachidonic Acid (100 μM) solution were added and the COX reaction was stopped by the addition of 50 μL of 1 M HCl after 2 min. $PGF_{2\alpha}$, produced from PGH_2 by reduction with stannous chloride was measured by enzyme immunoassay. This assay is based on the competition between PGs and a PG-acetylcholinesterase conjugate (PG tracer) for a limited amount of PG antiserum. The amount of PG tracer that is able to bind to the PG antiserum is inversely proportional to the concentration of PGs in the wells since the concentration of PG tracer is held constant while the concentration of PGs varies. This antibody–PG complex binds to a mouse anti-rabbit monoclonal antibody that had been previously attached to the well. The plate is washed to remove any unbound reagents and then Ellman's reagent, which contains the substrate to acetylcholine esterase, is added to the well. The product of this enzymatic reaction produces a distinct yellow color that absorbs at 410 nm. The intensity of this color, determined spectrophotometrically, is proportional to the amount of PG tracer bound to the well, which is inversely proportional to the amount of PGs present in the well during the incubation: Absorbance α [Bound PG Tracer] α1/PGs. Percent inhibition was calculated by the comparison of compound treated to various control incubations. The concentration of the test compound causing 50% inhibition (IC_{50}, μM) was calculated from the concentration–inhibition response curve (duplicate determinations).

4.2.2. Anti-inflammatory screening

The test compounds were evaluated using *in vivo* rat carrageenan-induced foot paw oedema model reported previously [21,26]. Male Sprauge–Dawley rats (250 gm body weight) were fasted with free access to water at least 16 h prior to experiments. Oedema was produced by injecting 0.2 mL of a solution of 1% λ-carrageenan in the hind paw. Paw volume was measured by water displacement with a plethysmometer (UGO BASILE) before, 1 and

2 h after treatment. The compounds were administered intraperitoneally with a 1 mL suspension of test compound in vehicle (0.5% methyl cellulose). Diclofenac and celecoxib were used as a standard drugs. The positive control group animals received the reference drug while the negative control received only the vehicle. The percentage was calculated by the following equation: anti-inflammatory activity (%) = (1-D/C)-100, where D represents the difference in paw volume before and after drug was administered to the rats, and C stands for the difference of volume in the control groups.

4.2.3. Analgesic screening

Male albino Swiss mice (25 gm body weight) were divided into various groups. Each mouse was initially placed on a hot plate thermostatically maintained at 58 °C [27–29]. The mouse was watched carefully for the time in seconds in which it displays nociceptive responses exhibited as licking or blowing its front paws. This time was considered as the control reaction time. A cut-off time of 60 s was used to avoid damage to the paws. To test the analgesic activity of the compounds each group of mice was treated with one dose of the test compounds (5–200 mg/kg, ip). The reaction time was then retested at 15, 30 and 60 min after injection (each animal acted as its own control). The percentage changes in the reaction were then calculated. The ED_{50} for each compound was then calculated by linear regression.

4.3. Docking methodology

Molecular modeling studies were performed with MOE 2008.10, software available from Chemical Computing Group Inc., 1010 Sherbrooke Street West, Suite 910, Montreal, QC.

4.3.1. Selection of protein crystal structure

Ligand-bound crystallographic structures of cyclooxygenase (COX-2) is available in the Protein Data Bank (http://www.rcsb.org/pdb/home/home.do). In this study, COX-2 complexed with SC-558 (1CX2) was evaluated and selected for docking. The errors of the protein were corrected by the structure preparation process in MOE. The first step in the generation of suitable protein structures is the assignment of hydrogen positions on the basis of default rules. All bound waters and cofactors contained in the PDB file have been removed. Finally, partial charges (the Gasteiger methodology) were calculated, and the active site of the ensemble has been defined as the collection of residues within 10.0 Å of the bound inhibitor and comprised the union of all ligands of the ensemble. All atoms located less than 10.0 Å from any ligand atom were considered.

4.3.2. Preparation of the ligand

The ligand coordinates were built using the builder tool of the MOE program. Next, the correct atom types (including hybridization states) and correct bond types were defined, hydrogen atoms were added, charges were assigned to each atom, and finally the structures were energy minimized (MMFF94x, gradient: 0.01) [48]. The energies of ligand structures were previously minimized using the semi-empirical AM1 method [49] with MOE program [36].

4.3.3. Docking experiment

The docking experiment on COX-2 (1CX2) was carried out by superimposing the energy minimized ligand on SC558 in the PDB file 1CX2, after which SC-558 was deleted. The default Triangle Matcher placement method was used for docking. GBVI/WSA dG scoring function which estimates the free energy of binding of the ligand from a given pose was used to rank the final poses. The ligand–enzyme complex with lowest S_score was selected.

Acknowledgments

The authors extend their appreciation to the Deanship of Scientific Research at King Saud University for funding the work through the research group project No. RGP-VPP-163.

Appendix A. Supplementary data

Supplementary data related to this article can be found at http://dx.doi.org/10.1016/j.ejmech.2014.12.039.

References

[1] S. Fiorucci, R. Meli, M. Bucci, G. Cirino, Biochem.. Pharmacol. 62 (2001) 1433.
[2] D.A. Williams, T.L. Lemke, Non-steroidal Anti-inflammatory Drugs, in: Foye's Principles of Medicinal Chemistry, fifth ed., Lippincott Williams& Wilkins, 2002, pp. 751–793.
[3] G. Dannhardt, W. Kiefer, G. Krämer, S. Maehrlein, U. Nowe, B. Fiebich, Eur. J. Med. Chem. 35 (2000) 499.
[4] B. Balaji, S. Hariharan, D.B. Shah, M. Ramanathan, Eur. J. Med. Chem. 86 (2014) 469.
[5] P. Sarnpitak, P. Mujumdar, C. Morisseau, S.H. Hwang, B. Hammock, V. Iurchenko, S. Zozulya, A. Gavalas, A. Geronikaki, Y. Ivanenkov, M. Krasavin, Eur. J. Med. Chem. 84 (2014) 160.
[6] S. Bansal, M. Bala, S.K. Suthar, S. Choudhary, S. Bhattacharya, V. Bhardwaj, S. Singla, A. Joseph, Eur. J. Med. Chem. 80 (2014) 167.
[7] J.R. Vane, Y.S. Bakhle, R.M. Botting, Ann. Rev. Pharmacol. Toxicol. 38 (1998) 9704.
[8] O. Laneuville, D.K. Breuer, D.L. DeWitt, T. Hla, C.D. Funk, W.L. Smith, J. Pharmacol. Exp. Ther. 271 (1994) 927.
[9] D.A. Kujubu, B.S. Fletcher, B.C. Varnum, R.W. Lim, H.R. Herschman, J. Biol. Chem. 266 (1991) 12866.
[10] L.J. Crofford, J. Rheumatol. 24 (Suppl. 49) (1997) 15.
[11] K. Seibert, Y. Zhang, K. Leahy, S. Hauser, J. Masferrer, W. Perkins, L. Lee, P. Isakson, Proc. Natl. Acad. Sci. 91 (1994) 12013.
[12] M.A.-A. El-Sayed, N.I. Abdel-Aziz, A.A.-M. Abdel-Aziz, A.S. El-Azab, Y.A. Asiri, K.E.H. ElTahir, Bioorg. Med. Chem. 19 (2011) 3416.
[13] M.A.-A. El-Sayed, N.I. Abdel-Aziz, A.A.-M. Abdel-Aziz, A.S. El-Azab, K.E.H. ElTahir, Bioorg. Med. Chem. 20 (2012) 3306.
[14] N.S. Buttar, K.K. Wang, Mayo Clin. Proc. 75 (2000) 1027.
[15] C. Michaux, C. Charlier, Mini-Reviews Med. Chem. 4 (2004) 603.
[16] T.D. Penning, J.J. Talley, S.R. Bertenshaw, J.S. Carter, P.W. Collins, S. Docter, M.J. Graneto, L.F. Lee, J.W. Malecha, J.M. Miyashiro, R.S. Rogers, D.J. Rogier, S.S. Yu, G.D. Anderson, E.G. Burton, J.N. Cogburn, S.A. Gregory, C.M. Koboldt, W.E. Perkins, K. Seibert, A.W. Veenhuizen, Y.Y. Zhang, P.C. Isakson, J. Med. Chem. 40 (1997) 1347.
[17] R.G. Kurumbail, A.M. Stevens, J.K. Gierse, J.J. McDonald, R.A. Stegeman, J.Y. Pak, D. Gildehaus, J.M. Miyashiro, T.D. Penning, K. Seibert, P.C. Isakson, W.C. Stallings, Nature 384 (1996) 644.
[18] T. Noguchi, R. Shimazawa, K. Nagasawa, Y. Hashimoto, Bioorg. Med. Chem. Lett. 12 (2002) 1043.
[19] H. Sano, T. Noguchi, A. Tanatani, Y. Hashimoto, H. Miyachi, Bioorg. Med. Chem. 13 (2005) 3079.
[20] A.A.-M. Abdel-Aziz, Eur. J. Med. Chem. 42 (2007) 612.
[21] A.A.-M. Abdel-Aziz, K.E.H. ElTahir, Y.A. Asiri, Eur. J. Med. Chem. 46 (2011) 1648.
[22] I.A. Al-Suwaidan, A.M. Alanazi, A.S. El-Azab, A.M. Al-Obaid, K.E. ElTahir, A.R. Maarouf, M.A. Abu El-Enin, A.A.-M. Abdel-Aziz, Bioorg. Med. Chem. Lett. 23 (2013) 2601.
[23] A.A.-M. Abdel-Aziz, A.S. El-Azab, S.M. Attia, A.M. Al-Obaid, M.A. Al-Omar, H.I. El-Subbagh, Eur. J. Med. Chem. 46 (2011) 4324.
[24] K.C. Nicolaou, C.J.N. Mathison, Angew. Chem. 44 (2005) 5992.
[25] M.J. Uddin, P.N. Praveen Rao, E.E. Knaus, Bioorg. Med. Chem. 12 (2004) 5929.
[26] C.A. Winter, E.A. Risely, G.W. Nuss, Proc. Soc. Exp. Biol. 111 (1962) 544.
[27] L. Ohlsson, Acta Pharmacol. Toxicol. (Copenh). 9 (1953) 322.
[28] G.E. Leighton, M.A. Johnson, K.G. Meecham, R.G. Hill, J. Hughes, Br. J. Pharmacol. 92 (1987) 915.
[29] H.A. Abdel-Aziz, K.A. Al-Rashood, K.E.H. ElTahir, G.M. Suddek, Eur. J. Med. Chem. 80 (2014) 416.
[30] S.M. Sondhi, R. Rani, P. Roy, S.K. Agrawal, A.K. Saxena, Bioorg. Med. Chem. Lett. 19 (2009) 1534.
[31] L.M. Lima, P. Castro, A.L. Machado, C.A. Fraga, C. Lugnier, V.L. de Moraes, E.J. Barreiro, Bioorg. Med. Chem. 10 (2002) 3067.
[32] J. Grover, V. Kumar, V. Singh, K. Bairwa, M.E. Sobhia, S.M. Jachak, Eur.J. Med. Chem. 80 (2014) 47–56.
[33] M.J. Uddin, A.V. Elleman, K. Ghebreselasie, C.K. Daniel, B.C. Crews, K.D. Nance, T. Huda, L.J. Marnett, ACS. Med. Chem. Lett. 5 (2014) 1254.
[34] O. Llorens, J.L. Perez, A. Palomer, D. Mauleon, Bioorg. Med. Chem. Lett. 9 (1999) 2779.
[35] R.M. Garavito, D.L. DeWitt, Biochem. Biophys. Acta 1441 (1999) 278.
[36] MOE, 10 of Chemical Computing Group Inc, 2008.

[37] R.G. Kurumbail, A.M. Stevens, J.K. Gierse, J.J. McDonald, R.A. Stegeman, J.Y. Pak, D. Gildehaus, J.M. Miyashiro, T.D. Penning, K. Seibert, P.C. Isakson, W.C. Stallings, Nature 384 (1996) 644.
[38] F. Chimenti, S. Vomero, Farm. Ed. Sci. 30 (1975) 884.
[39] K. Yoshiaki, T. Masumi, A. Kazuo, Chem. Pharm. Bull. 47 (1999) 529.
[40] B.B.C. Costa, R. Correa, M.M. De Souza, J.B. Pretto, J.V. Ardenghi, F. De Campos-Buzzi, F.V. Cechinel, Zeitschrift fuer Naturforschung C: J. Biosci. 62 (2007) 201.
[41] J. Kim, S.H. Hong, Org. Lett. 16 (2014) 4404.
[42] H. Takahashi, Acta Crystallogr. Sect. E Struct. Rep. Online 68 (2012) o2457.
[43] H. Tsubouchi, K. Tsuji, H. Ishikawa, Synlett 1 (1994) 63.
[44] T. Takata, Y.Z. Menceloglu, T. Endo, J. Polym. Sci. Part A: Polym. Chem. 30 (1992) 501.
[45] M.P. Costi, D. Tondi, M. Rinaldi, D. Barlocco, G. Cignarella, D.V. Santi, C. Musiu, I. Pudu, G. Vacca, P. La Colla, Eur. J. Med. Chem. 31 (1996) 1011.
[46] J. Zhang, M. Senthilkumar, S.C. Ghosh, S.H. Hong, Angew. Chem. 49 (2010) 6391.
[47] X.-F. Wu, S. Oschatz, M. Sharif, A. Flader, L. Krey, M. Beller, P. Langer, Adv. Synthesis Catal. 355 (2013) 3581.
[48] T.A. Halgren, J. Comp. Chem. 17 (1996) 490.
[49] M.J.S. Dewar, E.G. Zoebisch, E.F. Healey, J.J.P. Stewart, J. Am. Chem. Soc. 107 (1985) 3902.